



# GHG balance, its seasonality and response to soil type and management of northern agricultural grasslands: Eddy-covariance flux measurements from three adjacent fields in Finland



Narasinha Shurpali <sup>a,\*</sup>, Olli Peltola <sup>b</sup>, Yuan Li <sup>a</sup>, Petra Manninen <sup>a</sup>, Sanni Semberg <sup>a</sup>, Samuli Launiainen <sup>c</sup>, Arja Louhisuo <sup>a</sup>, Janne Rinne <sup>c</sup>, Mikko Järvinen <sup>a</sup>, Perttu Virkajärvi <sup>a</sup>, Pertti J. Martikainen <sup>d</sup>

<sup>a</sup> Grasslands and Sustainable Farming, Production Systems unit, Natural Resources Institute Finland, Halolantie 31A, Maaninka 71750, Finland

<sup>b</sup> Research infrastructure services unit, Natural Resources Institute Finland (Luke), Latokartanonkaari 9, Helsinki 00790, Finland

<sup>c</sup> Natural Resources Institute Finland (Luke), Bioeconomy and the Environment, Ecosystems and Modeling, Latokartanonkaari 9, Helsinki 00790, Finland

<sup>d</sup> Department of Environmental and Biological Sciences, University of Eastern Finland, Yliopistoranta 1, Kuopio 70211, Finland

## ARTICLE INFO

### Keywords:

Carbon sequestration  
Climate change mitigation  
Eddy covariance  
Grassland management

## ABSTRACT

Understanding how managed grasslands respond to climate and management regimes across global pedoclimatic zones is crucial to combating climate change. In this study, we used the eddy covariance method to continuously measure GHG fluxes from January through December 2022 at three boreal grassland sites in eastern Finland: Anttila on mineral soil, and Särkisuo and Pappilansuo on drained peat soils. Our results highlight significant seasonal variability and a strong dependence on management events (such as summer plowing at Pappilansuo, fertilization, and harvest at all three sites). The net CO<sub>2</sub> exchange ranged from a strong net uptake at Anttila ( $-2500 \text{ kg C ha}^{-1} \text{ yr}^{-1}$ ) and moderate uptake at Särkisuo ( $-500 \text{ kg C ha}^{-1} \text{ yr}^{-1}$ ) to net release at Pappilansuo ( $+930 \text{ kg C ha}^{-1} \text{ yr}^{-1}$ ). CH<sub>4</sub> fluxes were negligible at Anttila (total of  $+2 \text{ kg CH}_4 \text{ ha}^{-1} \text{ yr}^{-1}$ ) but reached  $+110 \text{ kg CH}_4 \text{ ha}^{-1} \text{ yr}^{-1}$  at Särkisuo and  $+51 \text{ kg CH}_4 \text{ ha}^{-1} \text{ yr}^{-1}$  at Pappilansuo. N<sub>2</sub>O emissions peaked after fertilization with  $+3.8$  (Anttila),  $+16$  (Särkisuo), and  $+29 \text{ kg N}_2\text{O ha}^{-1} \text{ yr}^{-1}$  (Pappilansuo). Anttila remained a net GHG sink at approximately  $-8.0 \text{ t CO}_2\text{-eq ha}^{-1}$ , whereas Särkisuo and Pappilansuo were net sources of  $5.0$  and  $12.3 \text{ t CO}_2\text{-eq ha}^{-1}$ , respectively. Anttila had the lowest GHG emissions per kilogram of grass biomass produced and had the highest yield, illustrating the potential for more climate-friendly grassland management on suitable soils. However, the organic soils showed higher GHG emissions. These results highlight the influence of soil type and the importance of management timing on the overall GHG balance in boreal grasslands.

## 1. Introduction

The rising levels of atmospheric greenhouse gases (GHGs) driven by industrial and agricultural expansion necessitate urgent actions to mitigate climate change impacts (Lee et al., 2024). Carbon dioxide (CO<sub>2</sub>), methane (CH<sub>4</sub>), and nitrous oxide (N<sub>2</sub>O) significantly contribute to global warming because of their potent effects on Earth's radiative balance (Dijkstra et al., 2012). International efforts, such as the "4 per mille Initiative," aiming at enhancing soil organic carbon by 0.4 % annually and potentially offsetting around 4 billion tons of CO<sub>2</sub> emitted each year, highlight the critical role of effective agricultural soil management in global carbon sequestration efforts (Minasny et al., 2017). In

line with this, the European Commission has set a target to reduce net GHG emissions by at least 55 % by 2030 compared to 1990 levels. This highlights the need for accurate measurements and management of GHG fluxes from the land-use sector to support sustainable practices and policy development effectively (European Commission, 2023).

Boreal grassland rotations managed for forage production for livestock, characterized by harsh climates and unique soil properties, present significant challenges and opportunities for sustainable agricultural management (Soussana et al., 2007; Norderhaug et al., 2023). These ecosystems in Nordic countries are influenced by past land-use and current agricultural practices, which intersect with the pressures of a changing climate, making their study especially pertinent (Forster et al.,

\* Corresponding author.

E-mail address: [narasinha.shurpali@luke.fi](mailto:narasinha.shurpali@luke.fi) (N. Shurpali).

2022; Grados et al., 2024). Northern Grasslands are crucial for their potential in carbon storage and GHG mitigation (Shurpali et al., 2009; Palosuo et al., 2015; Lind et al., 2019, 2020; Heimsch et al., 2021; Li et al., 2023). Despite efforts to quantify GHG fluxes at the plot and field scales, knowledge of the impacts of grassland management practices such as fertilization, harvest, and renovation is insufficient. Moreover, the comprehensive inclusion of all three major GHGs is frequently overlooked, limiting our understanding of the full spectrum of GHG emissions (Soussana et al., 2007; Dijkstra et al., 2012). Additionally, the influence of different soil types (mineral versus organic) on GHG dynamics in grasslands remains underexplored (Shurpali et al., 2009; Armolaitis et al., 2022).

High-time-resolution monitoring using the eddy covariance (EC) technique is essential for capturing the complex dynamics of GHG exchange at the field scale, offering insights into both long-term trends and episodic fluxes, which are critical for assessing the effectiveness of climate mitigation strategies (Soussana et al., 2007; Rebmann et al., 2018). Such detailed data are indispensable for refining GHG exchange models, which enhance the accuracy of GHG inventories and support the development of targeted management interventions. In this study, we examine the GHG flux data measured simultaneously by the EC method in three adjacent grasslands that are exposed to the same climatic conditions but differ in their soils and management regimes. The broad aim of this study is to enhance our understanding of GHG dynamics in northern managed grasslands. Specifically, we aim to 1) quantify how CO<sub>2</sub>, CH<sub>4</sub> and N<sub>2</sub>O fluxes, their seasonality and annual budgets vary between adjacent grasslands on mineral and drained peat soils; 2) reveal how net ecosystem exchange (NEE) and its components respond to grass canopy development and management (i.e. cutting, ploughing), 3) explore the impact of fertilization and ploughing on N<sub>2</sub>O flux dynamics, and 4) evaluate how mineral and organic grasslands differ in their GHG balance and grass yield under similar climate.

## 2. Materials and methods

### 2.1. Site characteristics and management practices

Field-scale CO<sub>2</sub>, CH<sub>4</sub>, and N<sub>2</sub>O fluxes representing the total GHG balance were measured during the 2022 year employing the EC technique at three distinct boreal agricultural grassland research sites, all located within a 3-kilometer radius near the Maaninka Research station, Natural Resources Institute Finland in Pohjois-Savo region in Finland.

**Table 1**  
Soil physical and chemical properties at the three study sites.

	Anttila		Särkisuo		Pappilansuo	
	Mean	Std. dev	Mean	Std. Dev	Mean	Std. Dev
Electrical conductivity (mS m <sup>-1</sup> ) <sup>a</sup>	0.6	0.1	2.4	0.9	1.1	0.2
pH <sup>b</sup>	5.8	0.2	5.5	0.2	5.3	0.1
Calcium (Ca, mg l <sup>-1</sup> ) <sup>a</sup>	1050	140	2425	332	1338	183
Phosphorus (P, mg l <sup>-1</sup> ) <sup>a</sup>	4.4	1.1	6.9	1.8	3.5	0.9
Potassium (K, mg l <sup>-1</sup> ) <sup>a</sup>	92.3	20.5	59.0	11.3	21.5	5.5
Magnesium (Mg, mg l <sup>-1</sup> ) <sup>a</sup>	139.4	39.0	313.2	75.3	149.3	30.9
Sulphur (S, mg l <sup>-1</sup> ) <sup>a</sup>	9.8	2.9	36.9	4.5	18.0	4.0
Cation exchange capacity (cmol kg <sup>-1</sup> ) <sup>a</sup>	9.6	1.5	24.0	1.9	14.3	1.5
SOC (0–10 cm), % <sup>a</sup>	3.36	0.82	38.9	11.1	27.0	4.1
Total N (0–10 cm), % <sup>a</sup>	0.24	0.07	1.9	0.4	1.9	0.3
C:N ratio	14.0		20.5		14.2	
Peat depth, cm (min, max)	—	—	63, > 100	—	25, 100	—

<sup>a</sup> Determined following ISO 11265: 1994, <sup>b</sup> ISO 10390: 2005, <sup>a</sup>Vuorinen and Mäkitie (1955), <sup>a</sup>In-house method JOK3016 (LECO) – Louhisuo et al. (2024)

Despite their proximity, these sites differ significantly in their soil physicochemical properties (Table 1) and management practices (Table 2). The mineral soil at the Anttila site (FI-Ant) is predominantly classified as Eutric Gleysol to Luvic Planosol/Stagnosol (IUSS Working Group WRB, 2007), a silt loam in texture according to the USDA classification system. The Särkisuo (FI-Sar) and Pappilansuo (FI-Pap) sites, located on drained organic soils primarily composed of sedge peat, vary in peat depth from 25 to over 100 cm. Särkisuo is nutrient-rich with better water retention, as indicated by soil electrical conductivity and nutrient contents (Table 1). Anttila is currently undergoing labeling process to become a Class 2 ecosystem station in ICOS (Integrated Carbon Observation System, Heiskanen et al., 2022) infrastructure.

### 2.2. Site management

#### 2.2.1. Anttila

The Anttila site has undergone several management activities that influenced soil/vegetation characteristics and potentially GHG emissions during the study year 2022. In May 2020, the site was ploughed and sown immediately afterwards with a mixture of timothy (*Phleum pratense*) - tall fescue (*Lolium arundinaceum*) and barley (*Hordeum vulgare*) as a cover crop. Barley was harvested in August 2020, followed by glyphosate application in September and autumn ploughing in November, leaving the soil bare over the winter of 2020–21. The following year, on June 3, 2021, the site was harrowed, sown, and fertilized with a mixture of red clover (*Trifolium pratense*) and timothy, and again including barley as a cover crop. One whole crop harvest was made on August 2, and the vegetation was left to overwinter, setting the stage for the 2022 measurement period. The management practices adopted during the study year are described in Table 2.

#### 2.2.2. Särkisuo

This site features a deep, nutrient-rich peat soil managed with specific fertilization and harvesting schedules to optimize grass growth. In 2020, the site was fertilized early in May and again in late June, grass harvesting was done in June and August. Glyphosate was applied in late September, and the field was left fallow over the winter. In June 2021, the site underwent a new management cycle, starting with ploughing, followed by sowing and fertilization with a mixture of wheat, oat, and grasses on June 9. The field was harvested as a whole crop in July.

#### 2.2.3. Pappilansuo

Operating under constraints due to landowner agreements and supporting natural grass and weed growth, the Pappilansuo site has served as a vegetative buffer zone to reduce nutrient and sediment leaching from the surrounding forested and agricultural area into adjacent waters. Management was limited to essential maintenance, with two grass cuts in July and September of 2020. From 2021 onwards, however, the site was used for forage production (grass under sown with wheat and oat mixture) and was first fertilized in mid-May, followed by a grass cut. To facilitate slow releasing potassium reserves in the soil, biotite was applied at the rate of 15 t ha<sup>-1</sup>. A second fertilization in June preceded the final grass cut in late July, after which the site was left to overwinter.

### 2.3. Eddy covariance and environment measurements

#### 2.3.1. Instrumentation setup

The EC systems measuring CO<sub>2</sub>, CH<sub>4</sub>, and N<sub>2</sub>O fluxes were standardized across the three sites to ensure consistency in data collection and alignment with community standards, particularly the protocols defining the practices used in the ICOS infrastructure (Nemitz et al., 2018; Rebmann et al., 2018). The measurement setup at each site included a sonic anemometer (uSonic-3 Cage MP, METEK GmbH, Germany) mounted on a tripod mast for observing the turbulent airflow. Gas concentrations were sampled using two separate analyzers at each site, with air inlets placed near the anemometer (horizontal separations of

**Table 2**

Site information and management practices conducted during the measurement year (2022).

		Anttila	Särkisuo	Pappilansuo
Site information	Coordinates	63.16347504° N, 27.23504448° E	63.15142822° N, 27.19906425° E	63.13808441° N, 27.24616241° E
	Elevation above sea level	92.2 m	84.8 m	89.2 m
	Soil type	Mineral	Drained organic	Drained organic
	Vegetation	Legume grassland	Mixed grasses	Mixed grasses
	Field parcel size	6.4 ha	7.1 ha	7.2 ha
	Measurement height	2.2 m	2.3 m	2.3 m
Management practices	Ditch preparation	—	10.03–17.03.2022	—
	First fertilization event	23.05.2022	30.05.2022	24.05.2022
	Amount applied (N kg ha <sup>-1</sup> )	52	90	84
	Herbicide against weeds	—	08.06.2022	17.06.2022
	First grass cut	21.06.2022	30.06.2022	27.06.2022
	Summer plowing	—	—	07.07.2022
	Second fertilization event	22.06.2022	04.07.2022	08.07.2022
	Amount applied (N kg ha <sup>-1</sup> )	44	69	69
	Reseeding	—	—	08.07.2022
	s grass cut	08.09.2022	15.08.2022	—
	Ditch preparation	—	03.08–15.08.2022	—

13 cm, 21 cm, and 16 cm at Anttila, Särkisuo, and Pappilansuo respectively). The analyzers used were the LI-7200RS (LI-COR Biosciences, USA) for CO<sub>2</sub> and H<sub>2</sub>O, and the TILDAS-CS (Aerodyne Research Inc., USA) for CH<sub>4</sub>, N<sub>2</sub>O, and H<sub>2</sub>O. The sampling systems included heated intake tubes of varying lengths and filters to maintain high flow rates and ensure data integrity. The inner diameter was 5.3 mm for the LI-7200RS and 6 mm for the TILDAS-CS. The tube length for the LI-7200RS was approximately 0.7 m at all sites. For the TILDAS-CS, the tube length was 11 m at Anttila, 14 m at Särkisuo, and 11 m at Pappilansuo. Gas concentrations were converted to dry mixing ratios during data logging at a frequency of 10 Hz. Data were continuously transferred to a remote storage system for subsequent processing. The CO<sub>2</sub> flux data covered the entire year of 2022 at all three sites. The CH<sub>4</sub> and N<sub>2</sub>O flux measurements began on May 6 at Särkisuo and March 4 at Pappilansuo. At Anttila, the CH<sub>4</sub> and N<sub>2</sub>O flux data spans the whole year.

Auxiliary meteorological and soil measurements were conducted continuously at the EC sites using harmonized instrumentation, and the data were logged at 1-minute intervals. These measurements included short- and longwave radiation components (CNR4 net radiometer, Kipp & Zonen B.V., The Netherlands), photosynthetic photon flux density (PPFD) (LI-190R Quantum Sensor, LI-COR Biosciences Inc., USA), air temperature and humidity (HMP155, Vaisala Oyj, Finland), precipitation (TR-525M Tipping Bucket Rain Gauge, Texas Electronics Inc., USA), and soil temperature and soil water content at depths of 5 cm, 10 cm, and 30 cm below the ground (HydraProbe, Stevens Water Monitoring Systems, Inc., USA).

### 2.3.2. Flux processing, gap-filling, and partitioning

EC data were processed with EddyPro version 7.0.7 following standardized procedures that were akin to the ICOS processing protocols (Sabbatini et al., 2018), similarly as in Tikkasalo et al. (2025). Gas fluxes were calculated with 30-min averaging time and turbulent fluctuations were separated from the observations using block averaging. Measured turbulent flow field was aligned with flow streamlines using sector-wise planar fitting (Rannik et al., 2020). The measurement setup (sampling tubes and filters) induced time lags between gas measurements and vertical wind and these time lags were estimated using cross-covariance maximization before calculating the covariances between turbulent vertical wind component and gas mixing ratios. The spectral losses due to dampening of the turbulent signal in the gas sampling lines and finite flux averaging interval were corrected following Fratini et al. (2012) and Moncrieff et al. (2005), respectively. However, the response times describing the high frequency attenuation were derived from cospectra between vertical wind and gas concentration fluctuations instead of power spectra of concentration fluctuations (Peltola et al., 2021).

The GHG flux time series were subsequently quality filtered

following (Vitale et al., 2020) with few modifications. First, flux observations were discarded from periods during which 1) fluxes exceeded predefined physically plausible range, 2) instruments were malfunctioning or 3) site diary indicated erroneous measurements. Then, the procedure of Vitale et al., (2020) was followed with the exception that the statistical model used in finding erroneous measurements was derived based on decomposing the time series with singular spectrum analysis and then reconstructing it with finite number of modes (Golyandina et al., 2001; Mahecha et al., 2007). As a last quality filtering step, low turbulence conditions, during which the EC fluxes do not represent ecosystem-atmosphere exchange, were identified using friction velocity ( $u_*$ ), and periods when  $u_*$  was below site-specific threshold were removed from the gas flux time series. After applying this quality filtering scheme, annual flux data coverage at Anttila was 63 %, 67 % and 67 % for CO<sub>2</sub>, CH<sub>4</sub> and N<sub>2</sub>O, at Särkisuo 58 %, 28 % and 30 % and at Pappilansuo 58 %, 43 % and 44 %, respectively. The lower coverage of CH<sub>4</sub> and N<sub>2</sub>O flux data at the organic soil sites was because these measurements did not start at the beginning of the year (Sect. 2.2.1.). Wherever necessary, the non CO<sub>2</sub> GHG fluxes were expressed in CO<sub>2</sub> equivalents using conversion factors of 27 for CH<sub>4</sub> and 273 for N<sub>2</sub>O corresponding to their global warming potential over a 100-year time horizon.

To estimate annual GHG fluxes, gaps in the GHG flux time series were filled first. Three machine learning (ML) algorithms were utilized: random forest (RF), extreme gradient boosting (XGB) and k-nearest neighbors (kNN) (see Supporting Info for more details). These three algorithms were selected due to their good performance in prior gap filling studies (e.g., Goodrich et al., 2021; Vekuri et al., 2023). “xgboost” (version 1.7.1) Python package was used to apply XGB method, whereas scikit-learn (version 1.1.1) functions “RandomForestRegressor” and “KNeighborsRegressor” were utilized in RF and kNN methods, respectively. For reducing the uncertainty stemming from selecting a specific gap filling algorithm, ensemble medians of the three gap filled time series were used in estimating the annual GHG balances and daily mean fluxes, whereas the spread among the three estimates gave a plausibility range for the annual GHG budgets. ML techniques were used to fill gaps between measurements, however at the organic soil sites (FI-Sar and FI-Pap) CH<sub>4</sub> and N<sub>2</sub>O flux measurements did not start from the beginning of the year and hence there were long gaps in these time series in the beginning of the year. These long gaps occurred outside growing season with small fluxes and hence they were filled with median fluxes observed during the December 2022. Gap filling long data gaps has been shown to be uncertain and hence we opted for this alternative approach for these longer gaps from the start of the year.

After gap filling, the measured net ecosystem exchange (NEE) of CO<sub>2</sub> between the atmosphere and the ecosystem was partitioned to

ecosystem respiration ( $R_{\text{eco}}$ ) and gross primary production (GPP) following the commonly used nighttime partitioning method (Reichstein et al., 2005) with slight modifications introduced by (Wutzler et al., 2018). However, unlike in Reichstein et al. (2005), here we forced nighttime GPP to zero by adding a 1.5 day running median of nighttime GPP to the GPP and  $R_{\text{eco}}$  time series and finally forced any residual nighttime GPP to zero. This adjustment aimed at fixing any inaccuracies in the partitioning method (GPP cannot depart from zero at night). It was ensured that after NEE partitioning the following relationship (Eq. 1) remained valid at each time step:

$$\text{NEE} = R_{\text{eco}} - \text{GPP} \quad (1)$$

To evaluate the dependence of GPP on LAI, a light response curve was fitted to GPP values obtained within a 4-day window surrounding the timing of each manual leaf-area index (LAI) measurement:

$$\text{GPP} = \frac{\alpha \beta \text{PPFD}}{\alpha \text{PPFD} + \beta} \quad (2)$$

where  $\alpha$  represents the apparent quantum yield and  $\beta$ , the GPP at light saturation. Non-linear least squares fits were utilized to obtain the values for  $\alpha$  and  $\beta$  for each 4-day window, and their dependency on LAI was assessed.

#### 2.4. Grass phenology and biomass yield

LAI was measured weekly during the growing season using a plant canopy analyzer (Lai2000, LiCor) with a 180° view cap. It was measured from plot trials established towards the edge of the field under the same management practices as on the whole field. Additionally, plant height was measured weekly, manually from the trial plots during the growing season.

An ecosystem-scale estimate for the (aerodynamic) canopy height and its temporal development was derived from the EC data following Chu et al. (2018). The method relies on logarithmic wind profile and on the notion that displacement height ( $d$ ) and roughness length ( $z_0$ ) depend on canopy height ( $h$ ). By assuming constant ratios between  $h$  and  $d$  and  $h$  and  $z_0$  (here  $z_0/h=0.1$  and  $d/h=0.6$  (Pennypacker and Baldocchi, 2016)),  $h$  can be solved from the logarithmic wind profile. Daily values for  $h$  were estimated with this method from data that fulfilled the following criteria: atmospheric stability parameter was between  $-0.05$  and  $0.05$  (near-neutral surface layer stability),  $u_*$  was between  $0.1$  and  $1$  m/s, ratio between standard deviation of vertical wind component and  $u_*$  was between  $1.1$  and  $1.5$  and the prevailing wind direction (WD) was from direction with several hundreds of meters of undisturbed grassland (at Anttila WD between  $290^\circ$  and  $20^\circ$ ; at Särkisuo WD between  $130^\circ$  and  $220^\circ$  and at Pappilansuo WD between  $300^\circ$  and  $40^\circ$ ). Daily canopy heights were estimated only when over 5 data points fulfilled these criteria. The aerodynamic canopy height, i.e. height of the canopy “sensed” by the turbulent flow, derived with this method typically matches well with the actual canopy height (Chu et al., 2018).

For estimating the grass biomass yield on a per ha basis, the study area was harvested with a harvester and baler mounted on a tractor. All bales were then weighed individually with a weighing scale on the baler. The dry matter content was determined by two independent replicate sampling of grass biomass from  $\frac{1}{4}$  of the bales with a standard bale sampler pipe and drying the biomass in  $60^\circ\text{C}$  for 48 h. Carbon and nitrogen content in biomass was determined from the dried samples by Eurofins Expert Services Finland laboratory.

### 3. Results

#### 3.1. Meteorological conditions

The Maaninka region received 588 mm precipitation in 2022, of

which 385 mm as rain during the snow free season. This annual precipitation amount was 29 mm less than the climatological normal (1991–2020) precipitation for the region (Jokinen et al., 2021). The mean annual temperature (MAT) in the region was  $4.6^\circ\text{C}$ , which is  $0.8^\circ\text{C}$  warmer compared to the long-term normal MAT. Soil temperature ( $T_{\text{soil}}$ , 5 cm depth) at the three grassland sites showed variable seasonal patterns (Fig. 1). In April,  $T_{\text{soil}}$  at mineral soil grassland site was lower (mean of  $2.9^\circ\text{C}$ ) compared to the other two sites. However, during May and July,  $T_{\text{soil}}$  at Anttila was higher, ranging from  $5.2$  to  $22.1^\circ\text{C}$ , in contrast to the more stable temperatures observed at the organic sites. Post-July,  $T_{\text{soil}}$  across all sites varied similarly. Photosynthetic photon flux density (PPFD), air temperature ( $T_{\text{air}}$ ) and vapor-pressure deficit (VPD) were similar at all sites due to their proximity and followed typical seasonal patterns in the region (Fig. 1). Soil water content SWC at 5 cm depth showed significant differences; Särkisuo (30–69 %) and Pappilansuo (40–70 %) fields on organic soils maintained higher volumetric moisture content throughout the year compared to the mineral soil grassland (10–39 %). At the organic sites, water table depth (WTD) was deepest at ca. 60 cm below the surface, and the variability from June to October was characterized by rapid increases after rainfall events, and slower recession caused by lateral tile drainage and evapotranspiration (ET). Temporal dynamics of WTD was similar at both sites, but at Pappilansuo WTD reached the surface after major rainfall events while it stayed deeper (below 10 cm depth) at Särkisuo (Fig. 1.), indicative of better drainage of the latter site.

#### 3.2. Grass phenology

The timing of vegetation height growth onset and subsequent height growth rate (Fig. 2) varied across the sites, and the total biomass yield was significantly higher at Anttila than at the other fields (Table 3). The correlation between measured plant height and aerodynamic canopy height was strong at Anttila ( $r^2 = 0.88$ , confidence interval, CI = 0.95), moderate at Särkisuo ( $r^2 = 0.69$ , CI = 0.95) and weak at Pappilansuo ( $r^2 = 0.14$ , CI = 0.95), reflecting differences in vegetation structure and its influence on the turbulent flow field, but also possibly imperfect spatial representativeness of manual grass height measurement locations (Fig. 2). LAI displayed patterns like the vegetation height, varying among the grassland sites and corresponding to harvests as expected (Fig. 3).

#### 3.3. $\text{CO}_2$ exchange and controlling factors

From the beginning of the year to the first week of May, the daily mean NEE, representing ecosystem respiration ( $R_{\text{eco}}$ ) during this part of the year, remained low (about  $0.5 \mu\text{mol m}^{-2} \text{s}^{-1}$ ). Subsequently, the daily mean NEE showed clear variations in response to phenological stages, harvesting, and other management practices at all sites (Fig. 3). At Anttila, we observed major peaks of negative NEE, one in mid- to late June and another in mid-July, corresponding to vigorous photosynthesis and rapid grass growth prior to each harvest (Table 2). Immediately after each harvest, the ecosystem switched from net uptake to a brief net  $\text{CO}_2$  release (positive NEE). Daily mean NEE ranged from a maximum uptake of about  $-9.3 \mu\text{mol m}^{-2} \text{s}^{-1}$  to a release of  $3.8 \mu\text{mol m}^{-2} \text{s}^{-1}$ . These patterns aligned well with LAI increases before cutting and the sudden removal of aboveground biomass afterward (Fig. 3).

At Särkisuo, a similar two-peak behavior was observed, with strong net  $\text{CO}_2$  uptake prior to each of the two harvests. Peak daily mean uptake rates reached about  $-7.8 \mu\text{mol m}^{-2} \text{s}^{-1}$ , while post-cutting NEE was as high as  $6.3 \mu\text{mol m}^{-2} \text{s}^{-1}$ . Compared to Anttila, the onset of  $\text{CO}_2$  uptake was slightly delayed in spring, which may be related to the peat soils being inundated with standing water and slower soil warming in peat. In contrast, the Pappilansuo site had only a single grass cut in late June. Peak net  $\text{CO}_2$  uptake ( $-9.7 \mu\text{mol m}^{-2} \text{s}^{-1}$ ) occurred just before that harvest. Immediately after this cutting, the field was ploughed and fertilized (following the “summer ploughing” practice) in early July to

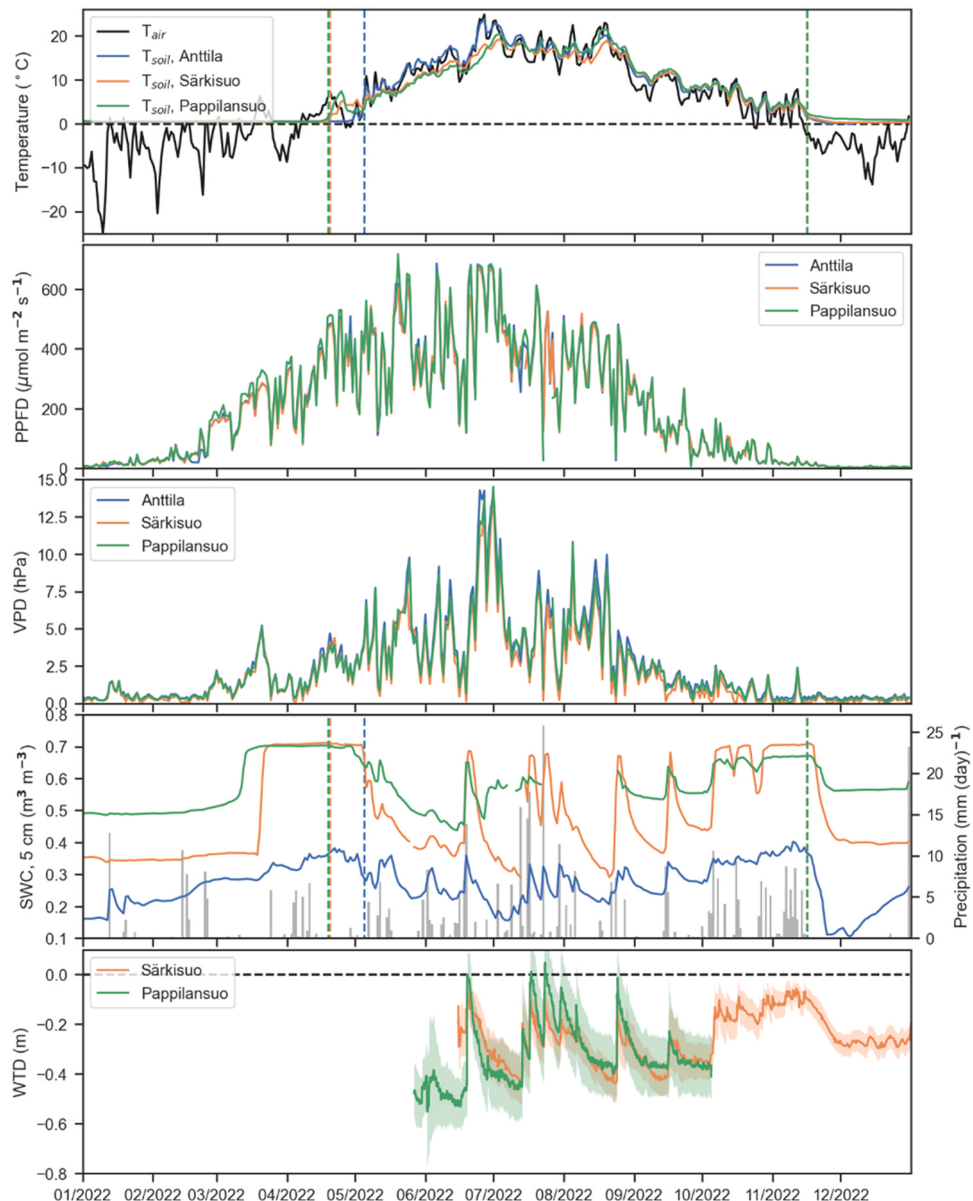


**Fig. 1.** Daily mean air ( $T_{air}$ ) and soil ( $T_{soil}$ ) temperature at 5 cm depth, photosynthetic photon flux density (PPFD), vapor pressure deficit (VPD), soil water content (SWC) at 5 cm depth, and daily precipitation and water table depth (WTD) below the soil surface at the three grassland sites in 2022. Vertical dashed lines show the snow-free period at each site.

establish new grass. This disturbance caused a switch to net  $\text{CO}_2$  loss, peaking at  $10.4 \mu\text{mol m}^{-2} \text{s}^{-1}$  daily mean  $\text{CO}_2$  emission from the field. About a week after the grass cut, tillage and fertilization at the Pappilansuo site,  $\text{CO}_2$  uptake began to recover and reached moderate uptake rates by late August. However, excessive wetness in September (high soil-water content, Figs. 1 and 3) prevented a second grass cut because the machinery could not be operated without damaging the field.

At Anttila, total annual GPP ( $12,600 \text{ kg (C) ha}^{-1} \text{ yr}^{-1}$ ) exceeded total  $R_{\text{eco}}$  ( $10,100 \text{ kg (C) ha}^{-1} \text{ yr}^{-1}$ ), making the site a net  $\text{CO}_2$  sink of  $-2500 \text{ kg (C) ha}^{-1} \text{ yr}^{-1}$  (Table 4). Särkisuo also remained a net  $\text{CO}_2$  sink ( $-500 \text{ kg (C) ha}^{-1} \text{ yr}^{-1}$ ), though both its GPP ( $9800 \text{ kg (C) ha}^{-1} \text{ yr}^{-1}$ ) and  $R_{\text{eco}}$  ( $9300 \text{ kg (C) ha}^{-1} \text{ yr}^{-1}$ ) were slightly lower. By contrast, Pappilansuo was a net  $\text{CO}_2$  source ( $930 \text{ kg (C) ha}^{-1} \text{ yr}^{-1}$ ), likely reflecting the prolonged period of bare soil conditions and ploughing disturbance in mid-summer, which fostered higher  $R_{\text{eco}}$  than GPP.

We assessed the uncertainty in the above reported  $\text{CO}_2$  budgets using three independent gap-filling algorithms. The spread in the resulting annual totals (Table 4) provides a measure of the methodological

uncertainty. Light-saturated level of GPP (Eq. 1) is a near linear function of LAI at all sites (Fig. 4), suggesting the harvests were conducted before major light limitation of photosynthesis emerged, or grass aging started to affect leaf-level photosynthetic uptake. The  $\beta$  increase with LAI is steepest at the Anttila site, indicative of a higher leaf-level photosynthetic capacity than at the drained peatland sites.

#### 3.4. $\text{CH}_4$ and $\text{N}_2\text{O}$ fluxes and their drivers

Daily  $\text{CH}_4$  fluxes significantly differed among the sites (Fig. 5). Särkisuo exhibited the highest daily average emissions (up to  $143 \text{ nmol m}^{-2} \text{s}^{-1}$  on peak days), consistent with its shallow water table and high peat content (Fig. 1, Table 1). Pappilansuo showed intermediate  $\text{CH}_4$  fluxes, whereas Anttila maintained near-zero or slightly positive  $\text{CH}_4$  fluxes throughout the year. Seasonally,  $\text{CH}_4$  fluxes from the two peat sites rose as soil temperature at 30 cm increased in late spring and summer, albeit there was strong seasonality in the  $\text{CH}_4$  emission temperature dependence (Fig. 6). On an annual basis, Särkisuo was the

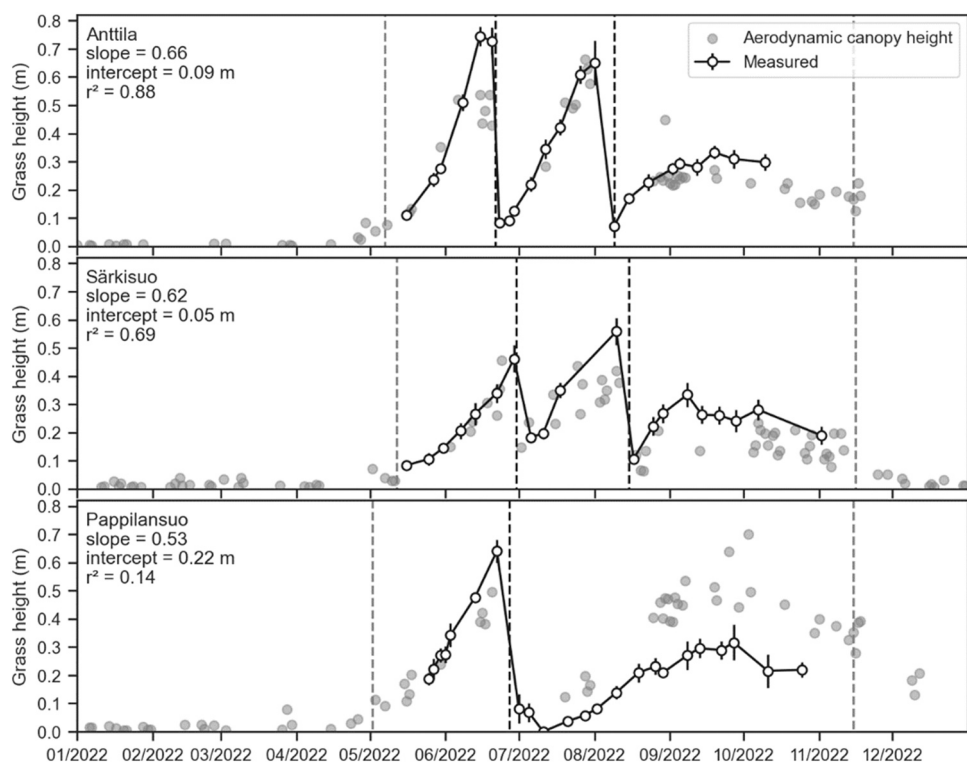


**Fig. 2.** Grass height at the three grassland sites. Grey markers show daily aerodynamic grass height estimated from the turbulence measurements (Sect 2.3). Black dashed lines denote harvest and grey dashed lines indicate snow melt and fall. Marker = mean; error bar = +/- standard deviation of independent samples.

**Table 3**

Annual fluxes at the three grassland sites during the year 2022. The range of annual flux estimates obtained with the different gap filling algorithms are given in parentheses.

	Anttila	Särkisuo	Pappilansuo
NEE (kg (C) ha <sup>-1</sup> yr <sup>-1</sup> )	-2500 (-2400...-2600)	-500 (-500...-600)	930 (860...1030)
R <sub>eco</sub> (kg (C) ha <sup>-1</sup> yr <sup>-1</sup> )	10100 (10100...10400)	9300 (8900...9900)	10810 (10610...10850)
GPP (kg (C) ha <sup>-1</sup> yr <sup>-1</sup> )	12600 (12500...12900)	9800 (9600...10500)	9870 (9570...9990)
CH <sub>4</sub> (kg (CH <sub>4</sub> ) ha <sup>-1</sup> yr <sup>-1</sup> )	2 (2...3)	110 (110...120)	51 (50...52)
N <sub>2</sub> O (kg (N <sub>2</sub> O) ha <sup>-1</sup> yr <sup>-1</sup> )	3.8 (3.7...4.0)	16 (16...17)	29 (28...29)

largest CH<sub>4</sub> source (110 kg (CH<sub>4</sub>) ha<sup>-1</sup> yr<sup>-1</sup>), followed by Pappilansuo (51 kg (CH<sub>4</sub>) ha<sup>-1</sup> yr<sup>-1</sup>) and Anttila (2 kg (CH<sub>4</sub>) ha<sup>-1</sup> yr<sup>-1</sup>) (Table 3).

We observed abrupt changes in the GHG exchange following the summer ploughing followed at the Pappilansuo site (Fig. 7). Prior to ploughing in July and after the grass harvest, the mean CO<sub>2</sub> flux was about 4  $\mu\text{mol m}^{-2} \text{s}^{-1}$  and that of CH<sub>4</sub> flux was about 7 nmol  $\text{m}^{-2} \text{s}^{-1}$  (Fig. 7). The summer ploughing done on July 7 temporarily enhanced both CO<sub>2</sub> and CH<sub>4</sub> release (Fig. 7a), but only for a few days after which CO<sub>2</sub> fluxes were above the pre-ploughing average values (Fig. 7a), while CH<sub>4</sub> fluxes dropped to near-zero (Fig. 7b) and well below the pre-ploughing CH<sub>4</sub> flux values for an extended period.

In contrast to CH<sub>4</sub>, fertilization, grass harvest, and precipitation events regulated the daily N<sub>2</sub>O fluxes (Figs. 5 and 8). Anttila showed minimal increase of N<sub>2</sub>O emissions after the first fertilizer application in late May (only ~0.18 % of applied N lost as N<sub>2</sub>O). However, the second fertilization (post-first cut) led to elevated emissions over 3–4 days,

including a peak of 17 nmol  $\text{m}^{-2} \text{s}^{-1}$  (daily average). Särkisuo showed higher N<sub>2</sub>O emissions following the first fertilization (2.4 % of the applied N lost as N<sub>2</sub>O) than the second (2.5 %), though the fluxes spanned a longer duration (9–10 days) for the first application. Daily average peak flux reached 34 nmol  $\text{m}^{-2} \text{s}^{-1}$ . Pappilansuo had the largest episodic daily N<sub>2</sub>O flux (54 nmol  $\text{m}^{-2} \text{s}^{-1}$ ) in mid-July, coinciding with the combination of the grass cut, ploughing, and fertilization on bare soil. All three sites were net N<sub>2</sub>O sources annually (Tables 3 and 4). Pappilansuo had the highest N<sub>2</sub>O emissions (29 kg (N<sub>2</sub>O) ha<sup>-1</sup> yr<sup>-1</sup>), followed by Särkisuo (16 kg (N<sub>2</sub>O) ha<sup>-1</sup> yr<sup>-1</sup>) and Anttila (3.8 kg (N<sub>2</sub>O) ha<sup>-1</sup> yr<sup>-1</sup>).

### 3.5. Annual GHG budgets and biomass yield

To facilitate comparison across all GHGs, we converted the annual CO<sub>2</sub>, CH<sub>4</sub>, and N<sub>2</sub>O fluxes to CO<sub>2</sub>-equivalents (CO<sub>2</sub>-eq) using the CH<sub>4</sub> and N<sub>2</sub>O global warming potentials over the 100-year time horizon (Table 4). Anttila sequestered about -9.1 t of CO<sub>2</sub>-eq ha<sup>-1</sup> and released 0.1 t CO<sub>2</sub>-eq ha<sup>-1</sup> as CH<sub>4</sub> and 1.1 t CO<sub>2</sub>-eq ha<sup>-1</sup> as N<sub>2</sub>O, leading to a net field-scale balance of -8.0 t CO<sub>2</sub>-eq ha<sup>-1</sup>. Särkisuo sequestered -2.1 t CO<sub>2</sub>-eq ha<sup>-1</sup> but emitted 2.8 t CO<sub>2</sub>-eq ha<sup>-1</sup> (CH<sub>4</sub>) and 4.3 t CO<sub>2</sub>-eq ha<sup>-1</sup> (N<sub>2</sub>O), ending with a net field-scale balance of 5.0 t CO<sub>2</sub>-eq ha<sup>-1</sup>. Pappilansuo emitted +12.3 t CO<sub>2</sub>-eq ha<sup>-1</sup> overall, with positive contributions from all three gases, largely driven by post-ploughing CO<sub>2</sub> releases and high N<sub>2</sub>O emissions.

Accounting for the removal of the harvested biomass as carbon lost from the fields, the net biome productivity (NBP) was positive at all sites, indicating that each field parcel lost carbon to the atmosphere (Table 4). The Anttila site produced the largest dry biomass yield, owing to high GPP supporting two grass cuts. Pappilansuo produced the least dry biomass, reflecting both the mid-summer ploughing and excess soil moisture during the autumn that prevented a second cut (Fig. 1, Table 2). Expressing NBP and total GHG emissions (in CO<sub>2</sub>-eq) per kilogram of harvested dry matter (animal feed CO<sub>2</sub>-eq) provides an LCA-type metrics such as of forage production efficiency (FPE) and GHG

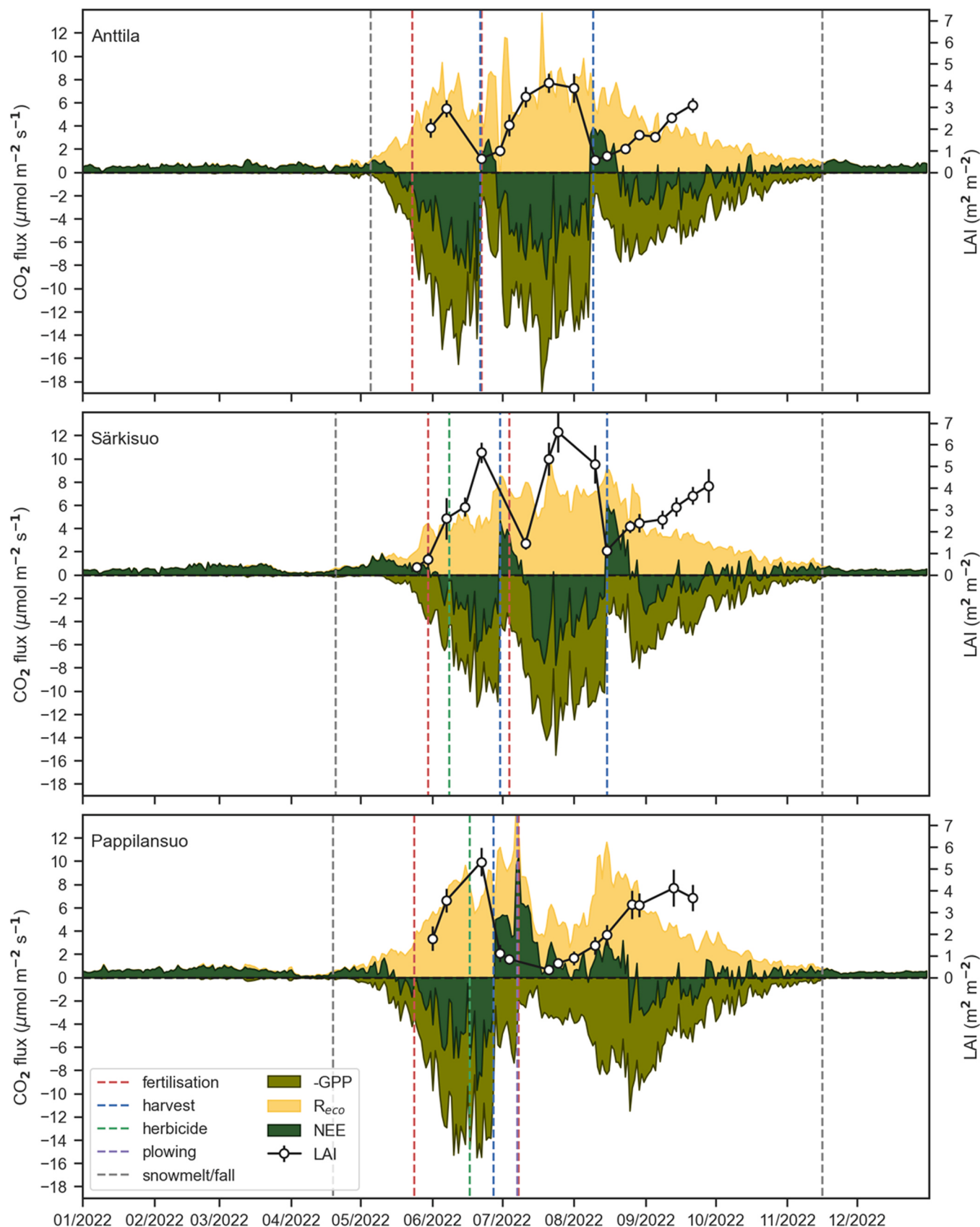


**Fig. 3.** Daily gross primary productivity (GPP), ecosystem respiration (Reco) and net ecosystem exchange (NEE=Reco-GPP) at the three grassland sites. Vertical dashed lines highlight the timing of different management practices. Leaf area index (LAI) is given with the markers (marker = mean; error bar = +/- standard deviation of independent samples).

**Table 4**

Annual GHG fluxes (columns 1–3), total GHG balance (column 4) and grass yield from Anttila, Särkisuo and Pappilansuo in 2022. Total GHGB is the sum of the three GHG fluxes expressed in CO<sub>2</sub> equivalents (conversion factors of 27 for CH<sub>4</sub> and 273 for N<sub>2</sub>O corresponding to global warming potential for 100-year time horizon were used), Grass C (column 5) expressed in % is the average carbon content of the harvested biomass, Grass yield (column 6) expressed in t ha<sup>-1</sup>, dry biomass yield (column 7) expressed in CO<sub>2</sub>-eq is calculated from grass yield as a function of C and moisture contents (data not shown here), NBP (net biome production in column 8) is calculated as the sum of annual CO<sub>2</sub> flux and dry biomass. The FPE (forage production efficiency, column 9) expressed in kg kg<sup>-1</sup> is the NBP in kg per kg of dry biomass produced. GHG emission intensity (GEI in column 10) is the ratio estimated as the GHGB (column 4) divided by the harvested biomass (column 6). GEI represents the emissions (sum of all three GHGs in CO<sub>2</sub> equivalents) in kg per kg of dry biomass produced at a given site. Based on NBP, the mineral soil site was more efficient in forage production (smaller FPE) and the least GHG emitter (negative GEI). The top row shows the numbered column names, the second row the units and the third row show how entities such as GHGB, Biomass, NBP, FPE and GEI were derived from the data in other columns of this table.

1. CO <sub>2</sub>	2. CH <sub>4</sub>	3. N <sub>2</sub> O	4. GHGB	5. Grass C	6. Yield	7. Biomass	8. NBP	9. FPE	10. GEI	
CO <sub>2</sub> -eq t ha <sup>-1</sup>			(1 + 2 + 3)	%	t ha <sup>-1</sup>	CO <sub>2</sub> -eq t ha <sup>-1</sup>	(6*5) * 44/12	(1 + 7)	kg kg <sup>-1</sup>	kg kg <sup>-1</sup>
1*	-9.1	0.1	1.0	-8.0	0.47	7.5	12.9	3.8	0.29	-1.1
2*	-2.1	2.8	4.3	5.0	0.47	4.7	8.2	6.1	0.74	1.1
3*	3.4	1.2	7.7	12.3	0.48	3.9	6.9	10.3	1.49	3.2

\*1 – Anttila site, 2\* – Särkisuo site and 3\* – Pappilansuo site

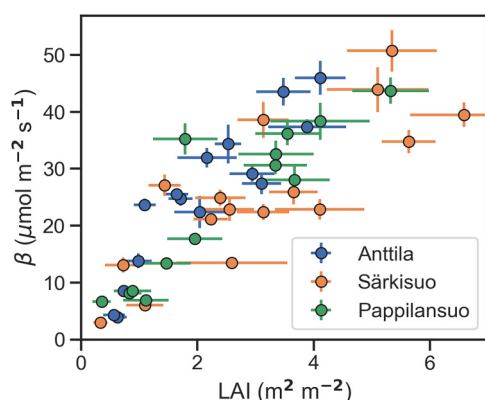


**Fig. 4.** CO<sub>2</sub> uptake in the Maaninka grasslands is driven by LAI and PPFD.

emission intension (GEI, Table 4). By that measure, Anttila had the lowest emissions intensity, which was 1/4 of that in Särkisuo and approximately 1/7 of that for Pappilansuo (Table 4).

#### 4. Discussion

Managed boreal grasslands are integral to the dairy and beef sectors

in these regions. They pose considerable challenges for climate change mitigation. Although the Finnish context underlies this study, grassland management on marginal or cold climates (e.g., Northern Europe, parts of Canada, Russia, and mountainous regions) often face similar constraints of short growing seasons, soil wetness, and potential peat drainage (Lohila et al., 2004; Soussana et al., 2007). Continuous EC measurements that capture all major GHG (CO<sub>2</sub>, CH<sub>4</sub>, and N<sub>2</sub>O) fluxes simultaneously are still scarce in such regions (Lohila et al., 2004; Heimsch et al., 2021, 2024; Gerin et al., 2023). Thus, our results offer insights relevant beyond Finland, highlighting how soil type (mineral vs. drained peat) and specific management practices strongly modulate GHG fluxes at field scale.

##### 4.1. Seasonal and soil-type effects on CO<sub>2</sub> dynamics

Our measurements reveal pronounced intra-seasonal variability in CO<sub>2</sub> fluxes, largely explained by crop phenology and management events (cutting, ploughing, fertilization). In the mineral soil grassland, net CO<sub>2</sub> uptake began quickly after snowmelt, whereas drained peat soils (Särkisuo, Pappilansuo) showed a slower onset of uptake in spring. Although peat soils can thaw earlier (due to topography, water accumulation, or lower albedo), they often remain colder or more waterlogged at the root zone (Van Huizen et al., 2020), potentially delaying early-season onset of GPP. Additionally, the large heat capacity and frequent high water content in peat may dampen temperature

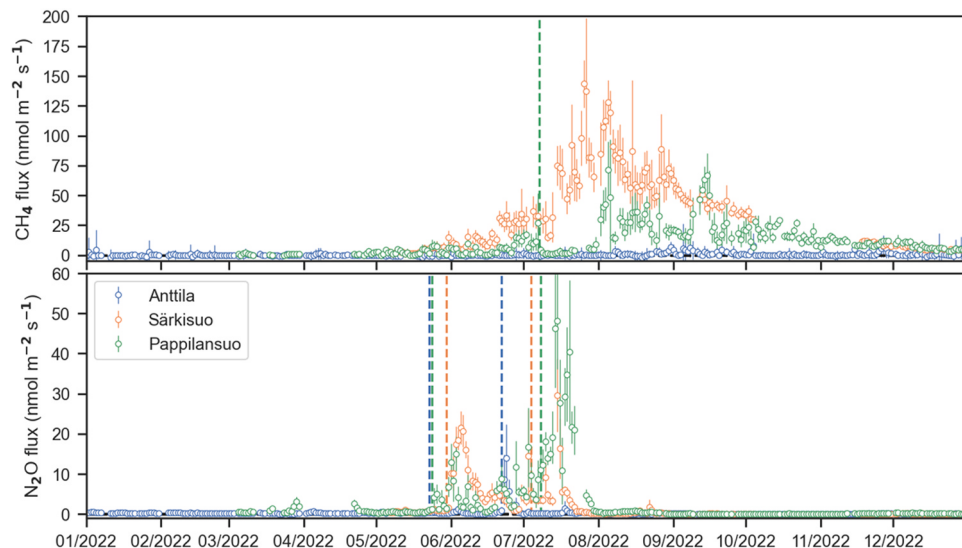


**Fig. 5.** Daily mean CH<sub>4</sub> and N<sub>2</sub>O fluxes at the three grassland sites. Top plot: dashed line shows the timing of plowing at Pappilansuo. Bottom plot: dashed lines relate to fertilization of the grassland fields. Daily means were calculated only if there were at least 10 measured flux values within the day.

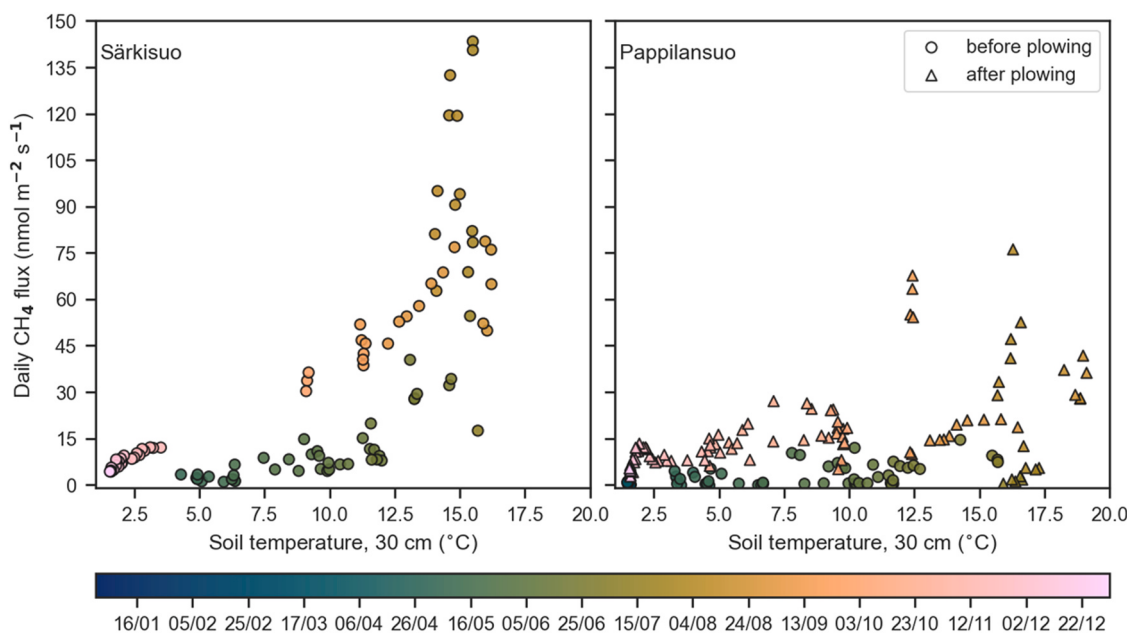


**Fig. 6.** Dependence of daily  $\text{CH}_4$  fluxes on soil temperature measured at 30 cm depth. Daily means were calculated only if there were at least 24 measured flux values within the day.

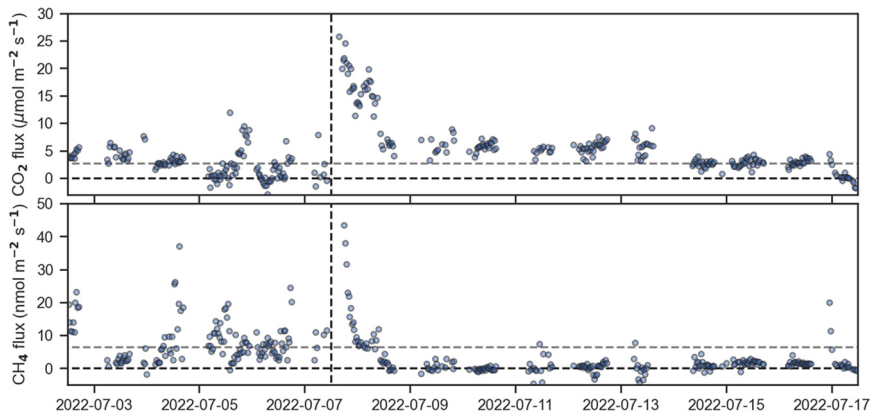


**Fig. 7.** (A)  $\text{CO}_2$  and (B)  $\text{CH}_4$  fluxes before and after ploughing the field at Pappilansuo during the 2022 growing season. Timing of the ploughing is marked with vertical dashed line. Horizontal grey dashed lines show the mean flux levels prior ploughing.

fluctuations (Różański and Stefaniuk, 2016), limiting root and microbial activity, annual net  $\text{CO}_2$  uptake (Fig. 3, Table 3), and showed the largest light-saturated GPP (Fig. 4), in part due to legume-based grass mixtures (red clover, timothy) that reduce external N-fertilizer demands (Sanz-Cobena et al., 2017; Lind et al., 2020). Särkisuo was a smaller net  $\text{CO}_2$  sink, with two grass cuts. Despite starting uptake later than at Pappilansuo, on an annual basis, this site captured more  $\text{CO}_2$  from the atmosphere. Pappilansuo was a net  $\text{CO}_2$  source following a single cut, summer ploughing, and re-seeding. Bare soil conditions in mid-summer promoted  $\text{Re}_{\text{CO}}$  that exceeded GPP. These annual results also reflect the phase of grassland rotation: newly ploughed peat fields can temporarily lose substantial amount of  $\text{CO}_2$  through enhanced SOC decomposition. Accounting for the C in harvested biomass as C lost from the ecosystems (expressed as NBP), all sites were annual  $\text{CO}_2$  sources (Table 4).

#### 4.2. $\text{N}_2\text{O}$ fluxes: role of moisture, fertilizer timing, and ploughing

$\text{N}_2\text{O}$  fluxes were most strongly influenced by fertilizer timing (Jones et al., 2017), precipitation, and soil aeration (Lind et al., 2019). In Anttila, early-season (cooler, drier) fertilization after spring thaw

produced a negligible  $\text{N}_2\text{O}$  peak. This is possibly due to the utilization of all available N by the plants to meet the demands of a vigorous growth in late May and early June. However, the post-harvest fertilization in Anttila led to a brief but significant  $\text{N}_2\text{O}$  peak. Generally, the second dose of fertilizer is applied soon after the first grass cut, owing to which, a major part of the active soil N depleting photosynthetic apparatus is removed from the field. Adding soil N when the demand for it is not high could lead to a part of the applied N being released episodically as  $\text{N}_2\text{O}$  to the atmosphere. The minimal loss of  $\text{N}_2\text{O}$  after the first fertilization in late May and high episodic release of  $\text{N}_2\text{O}$  following the post-harvest fertilization both hint at the role of above (plant associated) and below ground (rhizospheric microbial) processes in soil N dynamics and their role in mitigating agricultural  $\text{N}_2\text{O}$  emissions. These interactions also suggest that the farmers could perhaps delay the post-harvest N fertilization by a week or ten days allowing for some grass regrowth to happen so that the added N could be used better to boost the growth further and thus facilitate better N use efficiency and reduce the release of  $\text{N}_2\text{O}$  to the atmosphere. Also, a reason for low  $\text{N}_2\text{O}$  emissions from the Anttila site could be attributed to the presence of red clover as a legume crop that may have favored the complete denitrification leading to a

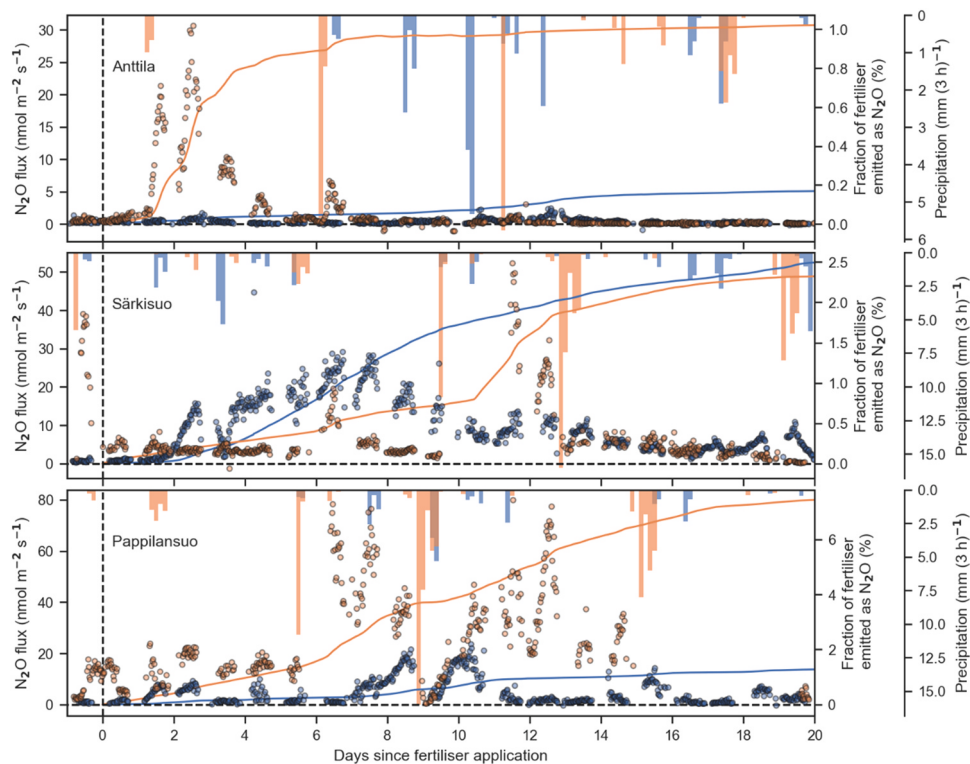


**Fig. 8.**  $\text{N}_2\text{O}$  fluxes after adding fertilizers at the three grassland fields. Markers:  $\text{N}_2\text{O}$  fluxes measured with EC. Lines: cumulative  $\text{N}_2\text{O}$  fluxes after fertilization normalized with the amount of fertilizer added to the field. Bars: Precipitation within 3 h intervals. Different colors refer to different fertilization events (blue: first fertilization, orange: second fertilization; see Table 2).

greater reduction of  $\text{N}_2\text{O}$  to  $\text{N}_2$  (Akiyama et al., 2016).

In Särkisuo, the first fertilization caused slightly larger  $\text{N}_2\text{O}$  emissions than the second, though both displayed ~2.4–2.5 % of the applied N lost as  $\text{N}_2\text{O}$  during the first 20 days after fertilization. Higher release of  $\text{N}_2\text{O}$  after the first fertilization in this field could be attributed to the delayed vegetation growth owing to high soil moisture in the early part of the season. At Pappilansuo, ploughing and fertilization on bare soil in July combined with rain events triggered large episodic  $\text{N}_2\text{O}$  release to the atmosphere. The absence of a developed crop canopy likely led to a lower plant N uptake, enabling higher  $\text{N}_2\text{O}$  fluxes (Regina et al., 2004; Sanz-Cobena et al., 2017).

The Intergovernmental Panel on Climate Change (IPCC) provides guidelines for countries to estimate  $\text{N}_2\text{O}$  emissions for reporting their national inventories. In 2019, the IPCC published a revised Tier 1 approach for estimating  $\text{N}_2\text{O}$  emissions that resulted in a Tier 1 emission factor (EF) of 1.6 % (1.3–1.9 %) for synthetic fertilizers (IPCC, 2019). Based on  $\text{N}_2\text{O}$  flux measurements made in this study, the emission factors estimated for 2022 for Anttila, Särkisuo and Pappilansuo sites are 2.4, 6.4 and 12.1 % N emitted as  $\text{N}_2\text{O}$  per kg N applied as synthetic fertilizers, respectively (refer to Supporting Table S1). Note that the Anttila site supported the cultivation of red clover as a legume crop in the grass mixture. Although we did not measure the rate per  $\text{ha}^{-1}$  of biological N fixation by red clover at our site, Anttila EF recalculated using an average biological N fixation rate for Finland of 102.5 kg N  $\text{ha}^{-1}$  following Nykänen et al. (2008) amounts to 1.2 % of the total N applied (96 kg of Synthetic N and 102.5 kg of biologically fixed N). The  $\text{N}_2\text{O}$  EF thus estimated for the mineral soil site was 25 % lower, while it was 400 % (Särkisuo) and 754 % (Pappilansuo) higher for the two drained peat grasslands in our study. The large variation in EFs estimated in this study suggests that the IPCC Tier 1 approach used in the national  $\text{N}_2\text{O}$  inventories needs to be refined yet for a well constrained global  $\text{N}_2\text{O}$  budget.

#### 4.3. $\text{CH}_4$ fluxes were large in peat soils

$\text{CH}_4$  fluxes were negligible in the well-drained mineral soil grassland but substantial in drained peat sites, especially Särkisuo. Emissions peaked in late July–August, coinciding with high soil temperature and shallow water table conditions (Lai, 2009; Huang et al., 2021). A strong hysteresis was observed in the Särkisuo  $\text{CH}_4$  flux temperature (measured at 30 cm depth) dependence indicating that there were also other factors controlling the  $\text{CH}_4$  flux seasonality, such as the availability of substrates for  $\text{CH}_4$  production (Chang et al., 2019). Another plausible explanation for the hysteresis could be that  $\text{CH}_4$  production took place deeper than at 30 cm depth and there was hysteresis between temperature at 30 cm depth and the depth where bulk of the  $\text{CH}_4$  was produced. Pappilansuo, despite being a drained peat field, showed lower total  $\text{CH}_4$  emissions than Särkisuo and even a transient drop in  $\text{CH}_4$  post-ploughing (Fig. 7b), which is likely due to temporary aeration and oxidation. At Särkisuo,  $\text{CH}_4$  fluxes were comparable to those reported for some pristine minerotrophic fens in Finland (Rinne et al., 2018, Rinne et al., 2020). Such high  $\text{CH}_4$  fluxes highlight the vulnerability of poorly drained agricultural peatlands to  $\text{CH}_4$  emissions. These findings on strong  $\text{CH}_4$  emissions are at odds with prior research suggesting that drained cultivated peat soils at worst are only minor  $\text{CH}_4$  sources even under poor drainage (e.g. Regina et al., 2004).

#### 4.4. Implications for sustainable management

Overall, Anttila exemplified a more climate-friendly grassland system: it had the lowest net field-scale GHG emissions (~8.0 t CO<sub>2</sub>-eq  $\text{ha}^{-1}$  yr<sup>-1</sup>) and the highest biomass yield among the three fields. In contrast, Särkisuo and Pappilansuo, both on drained peat soils, were net GHG emitters on an annual basis. It is worth noting here that the high feed CO<sub>2</sub>-eq for Pappilansuo is largely due to post-ploughing GHG emissions and hence ideally these metrics for production efficiency should be calculated using data over the full rotation cycle. Despite grassland

cultivation being one of widely adopted agricultural uses for organic soils abundant in Finland, especially in the northern part of the country, the findings suggest that substantial effort is still needed to optimize management (e.g., minimizing ploughing or refining fertilization schedules) to achieve climate-friendly outcomes. In Finland and elsewhere with agriculture on peat soils, alternative land uses such as rewetting (Kreyling et al., 2021) or paludiculture (Martens et al., 2023) may help curb CO<sub>2</sub> and CH<sub>4</sub> emissions. Other practical measures include: (1) optimized fertilizer application, precisely aligned nitrogen input with peak plant N demand could reduce fertilizer-driven N<sub>2</sub>O peaks (Jones et al., 2017); (2) minimal soil disturbance, reduced tillage or no-till could stabilize soil structure, reduce aeration pulses that promote decomposition, and mitigate CH<sub>4</sub> or N<sub>2</sub>O fluxes (Li et al., 2023; Hyväloma et al., 2024); (3) adapted cutting schedules; although multiple cuts can maintain high net primary productivity, caution is warranted if late-season wetness prevents harvest and leads to higher net emissions as in the case of peat soils as in this study, especially Pappilansuo.

## 5. Site GHG variability

This study elucidated the complex dynamics of CO<sub>2</sub>, CH<sub>4</sub>, and N<sub>2</sub>O fluxes in three boreal agricultural grasslands in Finland during 2022. The continuous, high-resolution GHG measurements helped us understand how seasonal climate, soil and vegetation types and grassland management practices regulate the ecosystem C and N flux dynamics. The mineral and drained peat soils responded differently to the spring onset. The snow on drained peat soils thawed 15–20 days earlier in the spring compared to the mineral soil grassland. The photosynthetic CO<sub>2</sub> uptake was initiated (implying GPP > 0) at the mineral soil grassland within two days of snow melt, while it took 13 and 22 days after snowmelt for the organic soils, Pappilansuo and Särkisuo, respectively to begin fixing atmospheric CO<sub>2</sub>. The net ecosystem CO<sub>2</sub> exchange at all sites varied with PPFD, LAI, temperature, grass growth, N fertilization and biomass harvesting. After each harvest, all ecosystems abruptly turned into CO<sub>2</sub> sources, before the post-harvest grass regrowth and simultaneously increasing GPP exceeded ecosystem respiration. While Anttila and Särkisuo sites allowed two grass cuts in the 2022 growing season, high soil moisture during autumn at the poorly drained Pappilansuo site prevented field machines from working allowing only a single grass cut at this site. Among the three sites, Anttila fixed the maximum amount of atmospheric CO<sub>2</sub>, Särkisuo was a smaller CO<sub>2</sub> sink while the Pappilansuo site was a source of CO<sub>2</sub> mainly owing to a sustained loss of CO<sub>2</sub> following the first and only grass cut, post-harvest summer ploughing and reseeding.

Mineral soil grassland emitted the lowest amount of CH<sub>4</sub>, while Pappilansuo was a moderate source and Särkisuo a strong source of CH<sub>4</sub> to the atmosphere. Soil temperature, water table level, soil moisture and labile carbon exudates in the grass rhizosphere owing to a rigorous grass growth during the middle of the season after a sluggish early growth (in Särkisuo), controlled methane emissions. The Anttila site supported a legume crop in the grass mixture and thus its requirement for N fertilizer was less compared to nonlegume grass species cultivated on drained peat soils. Hence, N<sub>2</sub>O emissions from this legume grass mixture were the lowest. The N<sub>2</sub>O seasonal variability at all three sites was characterized by low N<sub>2</sub>O emissions when fertilization was done during a period of active grass growth with a high demand for soil N. On the contrary, episodic, high release of N<sub>2</sub>O occurred during periods of low soil N demand (e.g., N fertilization soon after the first grass cut in Anttila and Pappilansuo and the first fertilization event in late May in Särkisuo when the grass growth was poor). High CH<sub>4</sub> and N<sub>2</sub>O emissions from the organic soil sites highlight the importance of measuring all the three GHG fluxes when evaluating the climate impacts of agricultural land use in such locations.

## 6. Conclusions

On annual basis, the mineral soil grassland had the highest forage production efficiency with the least amount of GHG emissions (in tons of CO<sub>2</sub>-eq) per ton of biomass produced, while the drained organic soil sites were less efficient with high net emissions of GHGs into the atmosphere. A complete, multi-year rotation-based life cycle analysis (LCA) would offer a more balanced emission profile as the high post-disturbance emissions may not persist annually, thus affecting the interpretation of per-ton feed emissions. Considering the high year to year variability associated with peat soil GHG emissions, high emissions observed in 2022 at Särkisuo and Pappilansuo may not represent typical annual conditions. Nevertheless, such emission patterns lead us to ponder whether grassland management on drained organic soils is sustainable from a climate perspective. Forage production on such soil types leads to high cost to the environment per liter of milk or kg of beef sold in the markets. For future studies, long-term studies across a broader range of boreal grassland sites, soil types, and management practices are essential to better capture the inter-annual variability and establish more robust, region-wide recommendations. Such research would better inform farm and landscape level grassland modelling, policy and farm-level decisions, supporting the dual goals of productive agriculture and climate change mitigation in boreal regions.

## CRediT authorship contribution statement

**Mikko Järvinen:** Writing – review & editing, Project administration, Funding acquisition. **Janne Rinne:** Writing – review & editing, Investigation, Conceptualization. **Arja Louhisuo:** Writing – review & editing, Validation, Methodology, Formal analysis. **Samuli Launiainen:** Writing – review & editing, Writing – original draft, Formal analysis, Conceptualization. **Olli Peltola:** Writing – review & editing, Writing – original draft, Visualization, Validation, Software, Methodology, Investigation, Formal analysis, Data curation, Conceptualization. **Shurpali Narasinha J.:** Writing – review & editing, Writing – original draft, Supervision, Resources, Project administration, Methodology, Investigation, Funding acquisition, Formal analysis, Conceptualization. **Pertti J. Martikainen:** Writing – review & editing, Validation, Resources, Formal analysis, Conceptualization. **Perttu Virkajärvi:** Writing – review & editing, Resources, Methodology, Funding acquisition. **Sanni Semberg:** Writing – review & editing, Methodology, Investigation, Formal analysis, Data curation. **Petra Manninen:** Data curation. **Yuan Li:** Writing – review & editing, Writing – original draft, Validation, Investigation.

## Disclaimer

The views and opinions expressed are those of the author(s) only and do not necessarily reflect those of the European Union. Neither the European Union nor the granting authority can be held responsible for them.

## Declaration of Competing Interest

The authors declare the following financial interests/personal relationships which may be considered as potential competing interests: Narasinha J. Shurpali reports financial support was provided by Finland Ministry of Agriculture and Forestry. If there are other authors, they declare that they have no known competing financial interests or personal relationships that could have appeared to influence the work reported in this paper.

## Acknowledgements

This work was supported by the Ministry of Agriculture and Forestry Finland (Project NC-GRASS: VN/28562/2020-MMM-2), The Academy of Finland (ENSINK project; Decision number 334422), the EU Horizon

2020 Framework Programme, EU H2020 Excellent Science (grant no. 101056921 “GreenFeedBack”). Olli Peltola acknowledges Research Council of Finland for funding (grant no. 354298). The authors acknowledge the technical support provided by Tero Toivonen and Ilpo Nuutinen (maintenance of EC flux towers) and several field staff (Hannu Raatikainen and Noora Granqvist (agronomic operations on the field) and Juliana Roivainen, Jenni Laakso and Arto Pehkonen (field sampling)) from the Grasslands and Sustainable Agriculture research group of Luke, Maaninka.

## Appendix A. Supporting information

Supplementary data associated with this article can be found in the online version at [doi:10.1016/j.agee.2025.109841](https://doi.org/10.1016/j.agee.2025.109841).

## Data availability

Data will be made available on request.

## References

- Akiyama, H., Hoshino, Y.T., Itakura, M., Shimomura, Y., Wang, Y., Yamamoto, A., Tago, K., Nakajima, Y., Minamisawa, K., Hayatsu, M., 2016. Mitigation of soil N2O emission by inoculation with a mixed culture of indigenous Bradyrhizobium diazoefficiens. *Sci. Rep.* 6 (1), 32869. <https://doi.org/10.1038/srep32869>, 10.1038/srep32869.
- Armalaits, K., Varnagirytė-Kabasinskienė, I., Žemaitis, P., Stakėnas, V., Beniusis, R., Kulbokas, G., Urbaitis, G., 2022. Evaluation of organic carbon stocks in mineral and organic soils in Lithuania. *Soil Use Manag.* 38, 355–368. <https://doi.org/10.1111/sum.12734>.
- Chang, K.-Y., Riley, W.J., Brodie, E.L., McCalley, C.K., Crill, P.M., Grant, R.F., 2019. Methane production pathway regulated proximally by substrate availability and distally by temperature in a high-latitude mire complex. *J. Geophys. Res.: Biogeosciences* 124 (6), 1715–1735. <https://doi.org/10.1029/2019JG005355>. <https://escholarship.org/uc/item/9v33z8km>.
- Chu, H., Baldocchi, D.D., Poindexter, C., Abrahma, M., Desai, A.R., Bohrer, G., Arain, M.A., Griffis, T., Blanken, P.D., O'Halloran, T.L., Thomas, R.Q., Zhang, Q., Burns, S.P., Frank, J.M., Christian, D., Brown, S., Black, T.A., Gough, C.M., Law, B.E., Lee, X., Chen, J., Reed, D.E., Massman, W.J., Clark, K., Hatfield, J., Prueger, J., Bracho, R., Baker, J.M., Martin, T.A., 2018. Temporal Dynamics of Aerodynamic Canopy Height Derived From Eddy Covariance Momentum Flux Data Across North American Flux Networks. *Geophys. Res. Lett.* 45, 9275–9287. <https://doi.org/10.1029/2018GL079306>.
- Dijkstra, F.A., Prior, S.A., Runion, G.B., Torbert, H.A., Tian, H., Lu, C., Venterea, R.T., 2012. Effects of elevated carbon dioxide and increased temperature on methane and nitrous oxide fluxes: evidence from field experiments. *Front. Ecol. Environ.* 10, 520–527. <https://doi.org/10.1890/120059>.
- European Commission, 2023. Land use sector – Climate Action. Directorate-General for Climate Action. Retrieved from [https://climate.ec.europa.eu/eu-action/land-use-sector\\_en](https://climate.ec.europa.eu/eu-action/land-use-sector_en).
- Forster, D., Helama, S., Harrison, M.T., Rotz, C.A., Chang, J., Ciaias, P., Pattey, E., Virkajarvi, P., Shurpali, N., 2022. Use, calibration and verification of agroecological models for boreal environments: A review. *Grassl. Res.* 1, 14–30. <https://doi.org/10.1002/glr2.12010>.
- Fratini, G., Ibrom, A., Arriga, N., Burba, G., Papale, D., 2012. Relative humidity effects on water vapour fluxes measured with closed-path eddy-covariance systems with short sampling lines. *Agric. For. Meteorol.* 165, 53–63. <https://doi.org/10.1016/j.agrformet.2012.05.018>.
- Gerin, S., Vekuri, H., Liimatainen, M., Tuovinen, J.-P., Kekkonen, J., Kulmala, L., Laurila, T., Linkosalmi, M., Liski, J., Joki-Tokola, E., Lohila, A., 2023. Two contrasting years of continuous N<sub>2</sub>O and CO<sub>2</sub> fluxes on a shallow-peated drained agricultural boreal peatland. *Agric. For. Meteorol.* 341, 109630. <https://doi.org/10.1016/j.agrformet.2023.109630>.
- Golyandina, N., Nekrutkin, V., Zhigljavsky, A.A., 2001. Analysis of time series structure. SSA and related techniques. CRC press.
- Goodrich, J.P., Wall, A.M., Campbell, D.I., Fletcher, D., Wecking, A.R., Schipper, L.A., 2021. Improved gap filling approach and uncertainty estimation for eddy covariance N<sub>2</sub>O fluxes. *Agric. For. Meteorol.* 297, 108280. <https://doi.org/10.1016/j.agrformet.2020.108280>.
- Grados, D., Kraus, D., Haas, E., Butterbach-Bahl, K., Olesen, J.E., Abalos, D., 2024. Common agronomic adaptation strategies to climate change may increase soil greenhouse gas emission in Northern Europe. *Agric. For. Meteorol.* 349, 109966. <https://doi.org/10.1016/j.agrformet.2024.109966>.
- Heimsch, L., Lohila, A., Tuovinen, J.P., Vekuri, H., Heinonsalo, J., Nevalainen, O., Korkiakoski, M., Liski, J., Laurila, T., Kulmala, L., 2021. Carbon dioxide fluxes and carbon balance of an agricultural grassland in southern Finland. *Biogeosciences* 18, 3467–3483. <https://doi.org/10.5194/bg-18-3467-2021>.
- Heimsch, L., Vira, J., Fer, I., Vekuri, H., Tuovinen, J.-P., Lohila, A., Liski, J., Kulmala, L., 2024. Impact of weather and management practices on greenhouse gas flux dynamics on an agricultural grassland in Southern Finland. *Agric. Ecosyst. Environ.* 374, 109179. <https://doi.org/10.1016/j.agee.2024.109179>.
- Heiskanen, J., Brümmer, C., Buchmann, N., Calfapietra, C., Chen, H., Gielen, B., Gkritzalis, T., Hammer, S., Hartman, S., Herbst, M., Janssens, I.A., Jordan, A., Juurola, E., Karstens, U., Kasurinen, V., Kruijt, B., Lankreijer, H., Levin, I., Linderson, M.-L., Loustau, D., Merbold, L., Myhre, C.L., Papale, D., Pavelka, M., Pilegaard, K., Ramonet, M., Rebmann, C., Rinne, J., Rivier, L., Saltikoff, E., Sanders, R., Steinbacher, M., Steinhoff, T., Watson, A., Vermeulen, A.T., Vesala, T., Vítková, G., Kutsch, W., 2022. The Integrated Carbon Observation System in Europe. *Bull. Am. Meteorol. Soc.* 103, E855–E872. <https://doi.org/10.1175/BAMS-D-19-0364.1>.
- Huang, Y., Ciaias, P., Luo, Y., Zhu, D., Wang, Y., Qiu, C., Goll, D.S., Guenet, B., Makowski, D., De Graaf, I., Leifeld, J., Kwon, M.J., Hu, J., Qu, L., 2021. Tradeoff of CO<sub>2</sub> and CH<sub>4</sub> emissions from global peatlands under water-table drawdown. *Nat. Clim. Change* 11, 618–622. <https://doi.org/10.1038/s41558-021-01059-w>.
- Hyväluoma, J., Niemi, P., Kinnunen, S., Brubbey, K., Miettinen, A., Keskinen, R., Soinne, H., 2024. Comparing structural soil properties of boreal clay fields under contrasting soil management. *Soil Use Manag.* 40, e13040. <https://doi.org/10.1111/sum.13040>.
- IPCC, 2019. Climate Change and Land: an IPCC special report on climate change, desertification, land degradation, sustainable land management, food security, and greenhouse gas fluxes in terrestrial ecosystems [C]P.R. Shukla, J. Skea, E. Calvo Buendia, V. Masson-Delmotte, H.-O. Pörtner, D.C. Roberts, P. Zhai, R. Slade, S. Connors, R. van Diemen, M. Ferrat, E. Haughey, S. Luz, S. Neogi, M. Pathak, J. Petzold, J. Portugal Pereira, P. Vyv, E. Huntley, K. Kissick, M. Belkacemi, J. Malley (C), (eds.)].
- IUSS Working Group WRB, 2007. World Reference Base for Soil Resources 2006, first update 2007. World Soil Resources Reports No. 103. FAO, Rome.
- Jokinen, P., Pirinen, P., Kaukoranta J.P., Kangas A., Alenius P., Eriksson P., Johansson M., Wilkman S., 2021. Climatological and oceanographic statistics of Finland 1991–2020. <https://doi.org/10.35614/isbn.9789523361485>.
- Jones, S.K., Helfter, C., Anderson, M., Coyle, M., Campbell, C., Famulari, D., Di Marco, C., van Dijk, N., Tang, Y.S., Topp, C.F.E., Kiese, R., Kindler, R., Siemens, J., Schrumpf, M., Kaiser, K., Nemitz, E., Levy, P.E., Rees, R.M., Sutton, M.A., Skiba, U. M., 2017. The nitrogen, carbon and greenhouse gas budget of a grazed, cut and fertilised temperate grassland. *Biogeosciences* 14, 2069–2088. <https://doi.org/10.5194/bg-14-2069-2017>.
- Kreyling, J., Tanneberger, F., Jansen, F., et al., 2021. Rewetting does not return drained fen peatlands to their old selves. *Nat. Commun.* 12, 5693. <https://doi.org/10.1038/s41467-021-25619-y>.
- Lai, D.Y.F., 2009. Methane Dynamics in Northern Peatlands: A Review. *Pedosphere* 19, 409–421. [https://doi.org/10.1016/S1002-0160\(09\)00003-4](https://doi.org/10.1016/S1002-0160(09)00003-4).
- Lee, H., Calvin, K., Dasgupta, D., Krinner, G., Mukherji, A., Thorne, P., Trisos, C., Romero, J., Aldunce, P., Ruane, A.C., 2024. CLIMATE CHANGE 2023 synthesis report summary for policymakers. CLIMATE CHANGE 2023 Synthesis Report: Summary for Policymakers.
- Li, Y., Korhonen, P., Kykkänen, S., Maljanen, M., Virkajarvi, P., Shurpali, N.J., 2023. Management practices during the renewal year affect the carbon balance of a boreal legume grassland. *Front. Sustain. Food Syst.* 7. <https://doi.org/10.3389/fsufs.2023.1158250>.
- Lind, S., Maljanen, M., Hyvönen, N.P., Kutvonen, J., Jokinen, S., Räty, M., Virkajarvi, P., Martikainen, P.J., Shurpali, N.J., 2019. Nitrous oxide emissions from perennial grass cropping systems on a boreal mineral soil. *Boreal Environ. Res.* 24, 215–232.
- Lind, S.E., Virkajarvi, P., Hyvönen, N.P., Maljanen, M., Kivimäenpää, M., Jokinen, S., Antikainen, S., Latva, M., Räty, M., Martikainen, P.J., Shurpali, N., 2020. Carbon dioxide and methane exchange of a perennial grassland on a boreal mineral soil. *Boreal Environ. Res.* 25, 1–17.
- Lohila, A., Aurela, M., Tuovinen, J.-P., Laurila, T., 2004. Annual CO<sub>2</sub> exchange of a peat field growing spring barley or perennial forage grass. *J. Geophys. Res. Atmospheres* 109. <https://doi.org/10.1029/2004JD004715>.
- Louhisuori, A., Yli-Halla, M., Termonen, M., Kykkänen, S., Jarvenranta, K., Virkajarvi, P., 2024. Long-term changes in soil phosphorus in response to fertilizer application and negative phosphorus balance under grass rotation in mineral soils in Nordic conditions (Article). *Soil Use Manag.* 40 (1), e13013. <https://doi.org/10.1111/sum.13013>.
- Mahecha, M.D., Reichstein, M., Lange, H., Carvalhais, N., Bernhofer, C., Grünwald, T., Papale, D., Seufert, G., 2007. Characterizing ecosystem-atmosphere interactions from short to interannual time scales. *Biogeosciences* 4, 743–758. <https://doi.org/10.5194/bg-4-743-2007>.
- Martens, H.R., Laage, K., Eickmanns, M., et al., 2023. Paludiculture can support biodiversity conservation in rewetted fen peatlands. *Sci. Rep.* 13, 18091. <https://doi.org/10.1038/s41598-023-44481-0>.
- Minasny, B., Malone, B.P., McBratney, A.B., Angers, D.A., Arrouays, D., Chambers, A., Chaplot, V., Chen, Z.-S., Cheng, K., Das, B.S., Field, D.J., Gimona, A., Hedley, C.B., Hong, S.Y., Mandal, B., Marchant, B.P., Martin, M., McConkey, B.G., Mulder, V.L., O'Rourke, S., Richer-de-Forges, A.C., Odeh, I., Padarian, J., Paustian, K., Pan, G., Poggio, L., Savin, I., Stolbovoy, V., Stockmann, U., Sulaeman, Y., Tsui, C.-C., Vägen, T.-G., van Wesemael, B., Winowiecki, L., 2017. Soil carbon 4 per mille. *Geoderma* 292, 59–86. <https://doi.org/10.1016/j.geoderma.2017.01.002>.
- Moncrieff, J.B., Clement, R., Finnigan, J., Meyers, T., 2005. Averaging, detrending, and filtering of eddy covariance time series. *Handbook of Micrometeorology: A Guide for Surface Flux Measurement and Analysis*. Springer, pp. 7–31. [https://doi.org/10.1007/1-4020-2265-4\\_2](https://doi.org/10.1007/1-4020-2265-4_2).
- Nemitz, E., Mammarella, I., Ibrom, A., Aurela, M., Burba, G.G., Dengel, S., Gielen, B., Grelle, A., Heinesch, B., Herbst, M., 2018. Standardisation of eddy-covariance flux measurements of methane and nitrous oxide. *Int. agrophysics* 32, 517–549.

- Norderhaug, A., Clemmensen, K.E., Kardol, P., Thorhallsdottir, A.G., Aslaksen, I., 2023. Carbon sequestration potential and the multiple functions of Nordic grasslands. *Clim. Change* 176, 55. <https://doi.org/10.1007/s10584-023-03537-w>.
- Nykänen, A., Jauhainen, L., Kempainen, Lindström, K., 2008. Field-scale spatial variation in soil nutrients and in yields and nitrogen fixation of clover-grass leys. *Agric. Food Sci.* 17, 376–393.
- Palosuo, T., Heikkilä, J., Regina, K., 2015. Method for estimating soil carbon stock changes in Finnish mineral cropland and grassland soils. *Carbon Manag.* 6, 207–220. <https://doi.org/10.1080/17583004.2015.1131383>.
- Peltola, O., Aslan, T., Ibrom, A., Nemitz, E., Rannik, Ü., Mammarella, I., 2021. The high-frequency response correction of eddy covariance fluxes – Part 1: An experimental approach and its interdependence with the time-lag estimation. *Atmos. Meas. Tech.* 14, 5071–5088. <https://doi.org/10.5194/amt-14-5071-2021>.
- Pennypacker, S., Baldocchi, D., 2016. Seeing the Fields and Forests: Application of Surface-Layer Theory and Flux-Tower Data to Calculating Vegetation Canopy Height. *Bound. Layer. Meteorol.* 158, 165–182. <https://doi.org/10.1007/s10546-015-0090-0>.
- Rannik, Ü., Vesala, T., Peltola, O., Novick, K.A., Aurela, M., Järvi, L., Montagnani, L., Mölder, M., Peichl, M., Pilegaard, K., Mammarella, I., 2020. Impact of coordinate rotation on eddy covariance fluxes at complex sites. *Agric. For. Meteorol.* 287, 107940. <https://doi.org/10.1016/j.agrformet.2020.107940>.
- Rebmann, C., Aubinet, M., Schmid, H., Arriga, N., Aurela, M., Burba, G., Clement, R., De Ligne, A., Fratini, G., Gielen, B., 2018. ICOS eddy covariance flux-station site setup: a review. *Int. Agrophysics* 32, 471–494.
- Regina, K., Syväsalo, E., Hannukkala, A., Esala, M., 2004. Fluxes of  $\text{N}_2\text{O}$  from farmed peat soils in Finland. *Eur. J. Soil Sci.* 55, 591–599. <https://doi.org/10.1111/j.1365-2389.2004.00622.x>.
- Reichstein, M., Falge, E., Baldocchi, D., Papale, D., Aubinet, M., Berbigier, P., Bernhofer, C., Buchmann, N., Gilmanov, T., Granier, A., Grünwald, T., Havráneká, K., Ilvesniemi, H., Janous, D., Knöhl, A., Laurila, T., Lohila, A., Loustau, D., Matteucci, G., Meyers, T., Miglietta, F., Ourcival, J.-M., Pumpanen, J., Rambal, S., Rotenberg, E., Sanz, M., Tenhunen, J., Seufert, G., Vaccari, F., Vesala, T., Yakir, D., Valentini, R., 2005. On the separation of net ecosystem exchange into assimilation and ecosystem respiration: review and improved algorithm. *Glob. Change Biol.* 11, 1424–1439. <https://doi.org/10.1111/j.1365-2486.2005.001002.x>.
- Rinne, J., Tuittila, E.-S., Peltola, O., Li, X., Raivonen, M., Alekseychik, P., Haapanala, S., Pihlatie, M., Aurela, M., Mammarella, I., Vesala, T., 2018. Temporal Variation of Ecosystem Scale Methane Emission From a Boreal Fen in Relation to Temperature, Water Table Position, and Carbon Dioxide Fluxes. *Glob. Biogeochem. Cycles* 32, 1087–1106. <https://doi.org/10.1029/2017GB005747>.
- Rinne, J., Tuovinen, J.-P., Klemmedsson, L., Aurela, M., Holst, J., Lohila, A., Weslien, P., Vestin, P., Łakomiec, P., Peichl, M., Tuittila, E.-S., Heiskanen, L., Laurila, T., Li, X., Alekseychik, P., Mammarella, I., Ström, L., Crill, P., Nilsson, M.B., 2020. Effect of the 2018 European drought on methane and carbon dioxide exchange of northern mire ecosystems, 20190517 Philos. *Trans. R. Soc. B* 375, 20190517.
- Rózański, A., Stefaniuk, D., 2016. On the prediction of the thermal conductivity of saturated clayey soils: Effect of the specific surface area. No. 4 *Acta Geodyn. Geomater.* 13 (184), 339–349. <https://doi.org/10.13168/AGG.2016.0016>.
- Sabbatini, S., Mammarella, I., Arriga, N., Fratini, G., Graf, A., Hörtnagl, L., Ibrom, A., Longdoz, B., Mauder, M., Merbold, L., 2018. Eddy covariance raw data processing for  $\text{CO}_2$  and energy fluxes calculation at ICOS ecosystem stations. *Int. Agrophysics* 32, 495–515.
- Sanz-Cobena, A., Lassaletta, L., Aguilera, E., Prado, Ad, Garnier, J., Billen, G., Iglesias, A., Sánchez, B., Guardia, G., Abalos, D., Plaza-Bonilla, D., Puigdueta-Bartolomé, I., Moral, R., Galán, E., Arriaga, H., Merino, P., Infante-Amate, J., Mejide, A., Pardo, G., Álvaro-Fuentes, J., Gilsanz, C., Báez, D., Doltra, J., González-Ubierna, S., Cayuela, M.L., Menéndez, S., Díaz-Pinés, E., Le-Noë, J., Quemada, M., Estellés, F., Calvet, S., van Grinsven, H.J.M., Westhoek, H., Sanz, M.J., Gimeno, B.S., Vallejo, A., Smith, P., 2017. Strategies for greenhouse gas emissions mitigation in Mediterranean agriculture: A review. *Agric. Ecosyst. Environ.* 238, 5–24. <https://doi.org/10.1016/j.agee.2016.09.038>.
- Shurpali, N.J., Hyvönen, N.P., Huttunen, J.T., Clement, R.J., Reichstein, M., Nykänen, H., Biasi, C., Martikainen, P.J., 2009. Cultivation of a perennial grass for bioenergy on a boreal organic soil – carbon sink or source? *GCB Bioenergy* 1, 35–50. <https://doi.org/10.1111/j.1757-1707.2009.01003.x>.
- Soussana, J.F., Allard, V., Pilegaard, K., Ambus, P., Amman, C., Campbell, C., Ceschia, E., Clifton-Brown, J., Czobel, S., Domingues, R., Flechard, C., Fuhrer, J., Hensen, A., Horvath, L., Jones, M., Kasper, G., Martin, C., Nagy, Z., Neftel, A., Raschi, A., Baronti, S., Rees, R.M., Skiba, U., Stefan, P., Manca, G., Sutton, M., Tuba, Z., Valentini, R., 2007. Full accounting of the greenhouse gas ( $\text{CO}_2$ ,  $\text{N}_2\text{O}$ ,  $\text{CH}_4$ ) budget of nine European grassland sites. *Agric. Ecosyst. Environ.* 121, 121–134. <https://doi.org/10.1016/j.agee.2006.12.022>.
- Tikkasalo, O.-P., Peltola, O., Alekseychik, P., Heikkilä, J., Laumiainen, S., Lehtonen, A., Li, Q., Martínez-García, E., Peltoniemi, M., Alekseychik, P., Tuominen, V., Mäkipää, R., 2025. Eddy covariance fluxes of  $\text{CO}_2$ ,  $\text{CH}_4$  and  $\text{N}_2\text{O}$  on a drained peatland forest after clearcutting. *Biogeosciences* 22, 1277–1300. <https://doi.org/10.5194/bg-22-1277-2025>.
- Van Huizen, B., Petrone, R.M., Price, J.S., Quinton, W.L., Pomeroy, J.W., 2020. Seasonal ground ice impacts on spring ecohydrological conditions in a western boreal plains peatland. *Hydrol. Process.* 34, 765–779. <https://doi.org/10.1002/hyp.13626>.
- Vekuri, H., Tuovinen, J.-P., Kulmala, L., Papale, D., Kolari, P., Aurela, M., Laurila, T., Liski, J., Lohila, A., 2023. A widely-used eddy covariance gap-filling method creates systematic bias in carbon balance estimates. *Sci. Rep.* 13, 1720. <https://doi.org/10.1038/s41598-023-28827-2>.
- Vitale, D., Fratini, G., Bilancia, M., Nicolini, G., Sabbatini, S., Papale, D., 2020. A robust data cleaning procedure for eddy covariance flux measurements. *Biogeosciences* 17, 1367–1391. <https://doi.org/10.5194/bg-17-1367-2020>.
- Vuorinen, J., Mäkitie, O., 1955. The method of soil testing in use in Finland, 63. *Agrogeological Publications*, pp. 1–44.
- Wutzler, T., Lucas-Moffat, A., Migliavacca, M., Knauer, J., Sickel, K., Sigut, L., Menzer, O., Reichstein, M., 2018. Basic and extensible post-processing of eddy covariance flux data with REddyProc. *Biogeosciences* 15, 5015–5030. <https://doi.org/10.5194/bg-15-5015-20>.